Asian Journal of Water, Environment and Pollution, Vol. 15, No. 4 (2018), pp. 15–26.
DOI 10.3233/AJW-180053

Investigation on Geological Structures of Alvand Region (Southeast of Zanjan City) in Iran

Mahdi Pouresmaieli, Arash Ebrahimabadi[1]*, Sahand Nouri[2] and Esmaeil Pouresmaeili[1]

Department of Mining Engineering, University of Zanjan, Zanjan, Iran
[1]Department of Mining, Qaemshahr Branch, Islamic Azad University, Qaemshahr, Iran
[2]Departmentof Geology, Maragheh Branch, Islamic Azad University, Maragheh, Iran
✉ Arash.xer@gmail.com

Received February 28, 2018; revised and accepted July 18, 2018

Abstract: Investigating geological structures plays a major role in economy of engineering projects such as petroleum and mining industries. Therefore, it is pivotal to study geological features. The study area is located in northwest of Qazvin Province and Tarom mountains. Tarom Mountains are located in Western Alborz as referred to in Iranian geological units which has a northwest-southeast trend and is located on the Upper Cretaceous-Cenozoic Magmatic belt. This volcanic-plutonic belt has a northwest to southeast trend. The volcanic and intrusive units of the region that belong to Karaj Formation is composed of two members called Amand and KordKand that are affected by alpine orogeny movements. Different folds were geometrically analyzed in the region and based on the mapping of the data on the Schmidt network and the flute (1964) and Rickard (1971) charts; they were categorized as gently to moderate plunging and steeply inclined folds. Based on Twiss's classification of folds (1988), findings showed most folds are sub-angular and in terms of the appearance ratio are in broad type. Using Ramsay's (1967) classification and the pattern variation of the contour lines for some folds, they are all in category 1 and mostly in category 1B which can be considered as a flexural-slip mechanism. The results demonstrated that the process of all the axial surfaces and the axis of folds are generally in the direction of northwest-southeast. The faults taken from the study area are mostly reverse and strike-slip in the direction of northwest-southeast in accordance with the western Alborz.

Key words: Geological structure, fault, fold, Alvand, Zanjan.

Introduction

The Alborz Mountains are located in northern Iran and are part of the Alpine-Himalayan orogeny belt in West Asia. This mountain range is located in the south of Caspian Sea, causing the separation of the northern margin of our country and central Iran. This mountainous belt has an arc with 2000 kilometres length which begins in the small Caucasus in the Republic of Azerbaijan and ends in the mountains of Paropamisus in Afghanistan (Alavi, 1996). Many researchers have studied the structural characteristics of the Alborz and presented different views on how it originated and evolved. However, due to some reasons such as lack of economic justification and its rough topography very limited structural studies have been conducted in this region so far. In the present study, we have tried to examine the structural features of a small part of this mountain range which is located in the north of Eastern Alborz. The results of this study can provide

*Corresponding Author

basic information for being used in studies that are conducted to identify the characteristics and structural development of Alborz.

This region has a geological and structural background similar to the entire Alborz as it is located in the north-eastern part of the Alborz; therefore, it is preferred to first give a brief overview of the structural studies and models presented for Alborz. The first study of the Alborz was conducted in 1968, in which Stocklin provided a structural model and assumed that Alborz was in form of a syncline; the same person based on his findings plotted the first cross section of the Alborz later on Stocklin (1968). In 1990, Şengör used the mentioned model and after completing it, described Alborz as an asymmetric flower shaped structure that tends towards south. Alavi (1991, 1996) proposed another model and assumed Alborz as a complex anticline. In fact, in his structural model, he assumed Alborz as a fault-related folding belt of thin crust consisting of numerous thrust layers and duplex.

The operation of these structures results in the rise of rock sequences and the formation of a compound vault. Axen et al. (2001), after studying the thrust faults in Alborz, interpreted the mountain range as a flower shaped transpression structure with a tendency towards south as Şengör had already referred to it. Axen et al. (2001) believes that the reason behind this tendency towards south is the movement of a floating continental crust from the south side that is going under Alborz. Other people in the years following Alavi's studies and modelling have made comments with little difference, including the work of Allen et al. (2003). According to him, a general landslide between the thrust faults and left lateral strike slip faults has been distributed, and as a result he considers Alborz as a left lateral transpression belt (Figure 1).

Guest et al. (2006, 2007), after extensive studies in Alborz, attributed the contact of Arabian block and the active Iranian-Turkish margin to middle Miocene. They investigated the deformation of the Alborz Mountains 3-5 km far from the Southern Caspian Basin as well as Central Iran from the Miocene to the present time. Each zone was about 10 and 3-6 km long respectively. In addition, Alborz is considered a simple folding in the north of Iran, and its situation is similar to the early stages of the continental-oceanic collision (Southern Caspian Basin). They also rejected the cross section along the southern Caspian basin-central Iran and the arch model with a thin crust deformation for the Alborz, and supported the ideas of Allen et al. (2003). In contrast to Alavi (1996), which considers the structure of entire Alborz to be made of thin crust tectonics, Guest et al. (2007) believe that the thin crust tectonics can be expanded only to a limited area of the Alborz, and not to its entirety. Ehteshami-Moinabadi (2016) attempts to compile available geologic, air-borne magnetic and seismic data with other forms of evidence to introduce some certain and potential TB faults in the Alborz Range from Talesh Mountain to west Central Alborz between 48° and 51° eastern longitudes. Mattei et al. (2017) defined the rotational history of the Alborz mountain belt, leading to yield the tectonic and paleogeographic evolution of northern Iran in the framework of Arabia-Eurasia continental deformation for the first time. There are some notable attempts to investigate and model the structural features in Iran (Adib et al., 2017; Bayet-Goll et al., 2016).

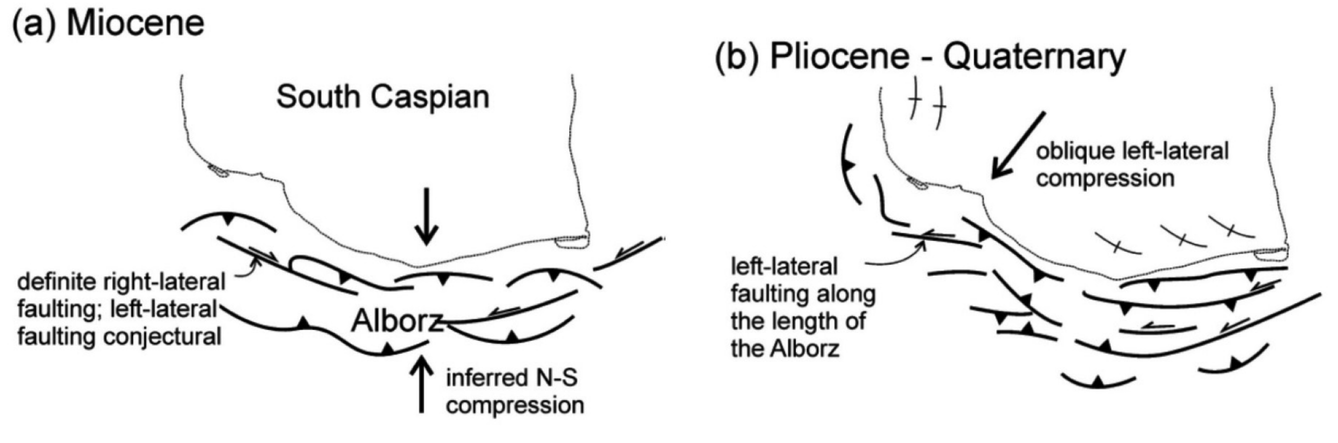

Figure 1: Alborz structural evolution in Cenozoic. (A) Miocene, a compression deformation which is in relation with left and right lateral strike-slip faults and the only existing fault are the active right lateral faults. (B) Pliocene-quaternary, a compressive deformation which is in relation with left lateral strike slip faults in Alborz. (Allen et al., 2003)

Due to the lack of complete and accurate data from the structural zones and the complexity of the structures process, the present study aims at identifying and analyzing the structures of the region, identifying possible relationships between structures and investigating the relationship between the structures of the region and the tectonic of Iran. To achieve this goal and to provide a structural evolution model for the region, the following activities have been carried out: Collecting and studying previous works in the area, such as articles, theses, pictures and maps; preparing and studying satellite images to identify and recognize the structures of the study area; field investigation to measure structural features (faults and folds) by geological compass; preparation and drawing the structural map of the study area; and structural analysis by software (GEOrient and Stereonet software for displaying data and finding the Paleostress axes, which ultimately leads to the analysis of the structural data of the study area).

The Study Area

The study area is located in 76 km south-east of Zanjan province in the most northwestern part of Qazvin province. Within the framework of the study, Zanjan Map 1: 250,000 with an approximate area of 400 sq. km, to the coordinates of 36 degrees, 30 minutes to 36 degrees and 45 minutes north latitude, and 49 degrees and 15 minutes to 49 degrees and 30 degrees of eastern longitude (Figure 2).

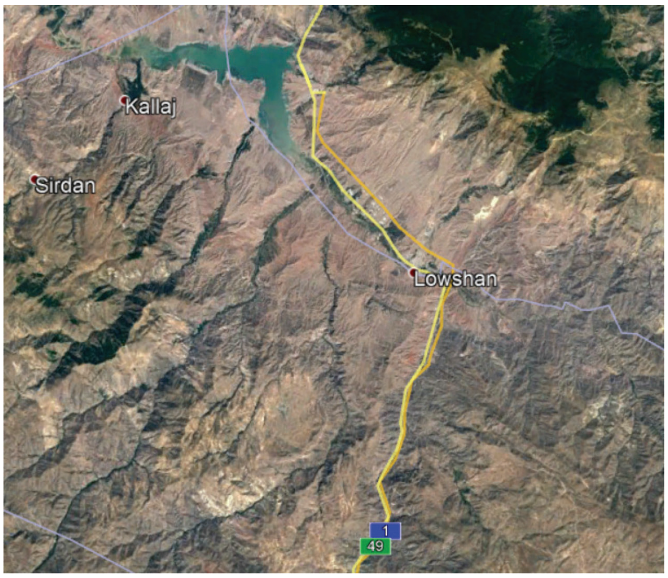

Figure 2: Geographical location of the study area.

The Alborz mountain range is located in northern Iran and is part of the Alpine-Himalayan Orogeny belt in West Asia. This mountain range is located in the south of the Caspian Sea, causing the separation of the northern margin of Iran and Central Iran. This mountainous belt has an arc with a length of 2000 kilometre, which begins in the small Caucasus in the Republic of Azerbaijan and ends in the mountains of Paropamisus in Afghanistan (Alavi, 1996). Noticeable folding, complex tectonics, and high altitudes are important features of the geomorphology of this region. Most of the facies in the region mainly belong to the Eocene and Tertiary facies. The diversity of these units in terms of material and erosion factor have created a variety of topographic levels that can be divided into three major groups: (1) low elevation regions, (2) semi-high regions and (3) highlands.

Material and Methods

Since the present study favours the applied research type, so the research method has been a combination of library studies, studying the satellite imagery and photos, field observations, designing the structural maps of the study area, and analyzing the data using Stereonet and GEOrient software.

In the present study, landsat7 satellite imagery was used to investigate and prospect the lineaments of the region. The models that have been employed in this method are as follows: Digital terrain model, digital elevation model, and height shadow patterns on the DEM. In the process of investigating the faults, the density of faults was designed using the Landsat map and the indicated model. Then, the density of faults was combined in the GIS environment and the associated lineaments were linked together. Finally, the rose diagram was designed by calculating the azimuth of the lineaments.

In the process of studying the folds and after recording the data that was obtained from the folds' limbs, the classification was conducted based on the position of the central axis of folds and using the Ramsay (1967) diagram. The angle between the limbs was determined by Donath et al. (1964). The style of the fold, the appearance ratio, and the degree of the fold's vertex was determined by Twiss (1988) and their geometric analysis was performed based on Twiss (1988) and Ramsay (1967). The anticlines and synclines were identified and then classified based on the geometric characteristics of the folds, types of folds, and rankings of Ramsay (1967). Added to that, the analysis of the type of folds was conducted based on the angle of plunge and the distribution diagrams of the folds were designed based on Rickard (1971).

Geology of the Study Area

Most of the outcrops of the north of Zanjan province are pyroclastic collections of Eocene (Karaj Formation), which are divided into two sections of Amand and KordKand. The predominant petrology of the pyroclastic rocks of the northern part of the province, like other parts of the Alborz, is a type of green tuff with intermediate layers of Chile and sometimes limestone that has a shape of curved belt to the right. Apart from the pyroclastic rocks, there are also andesitic lavas, basaltic andesite, rhodizite-porphyry and non-porphyry that are formed both in the sea and land. The sedimentary forms found in pyroclastics and volcano classics such as bedding, gradual gradation, bent lamination, flute-casts, and gravity slides not only indicate the accumulation in the marine environment, but also some kind of turbulent flows and tectonic turmoil in the times of deposition. Existing evidence suggests that during a tectonic subsidence the Neogene sediments are accumulated in the Talesh Mountains in the north and Tarom Mountains in the south. In Zanjan province, the areas located in south of Tarom Mountains are part of Central Iran's plate and as a result of this operation the northeast-southwest faults have changed into several tectonic blocks which are limited to fault zones, the most important of which are: (A) Zanjan-Abhar subsidence, (B) Soltanieh horst, (C) Kavand-Doteppeh depression and (D) Said Abad-Karasf Hills (Figure 3).

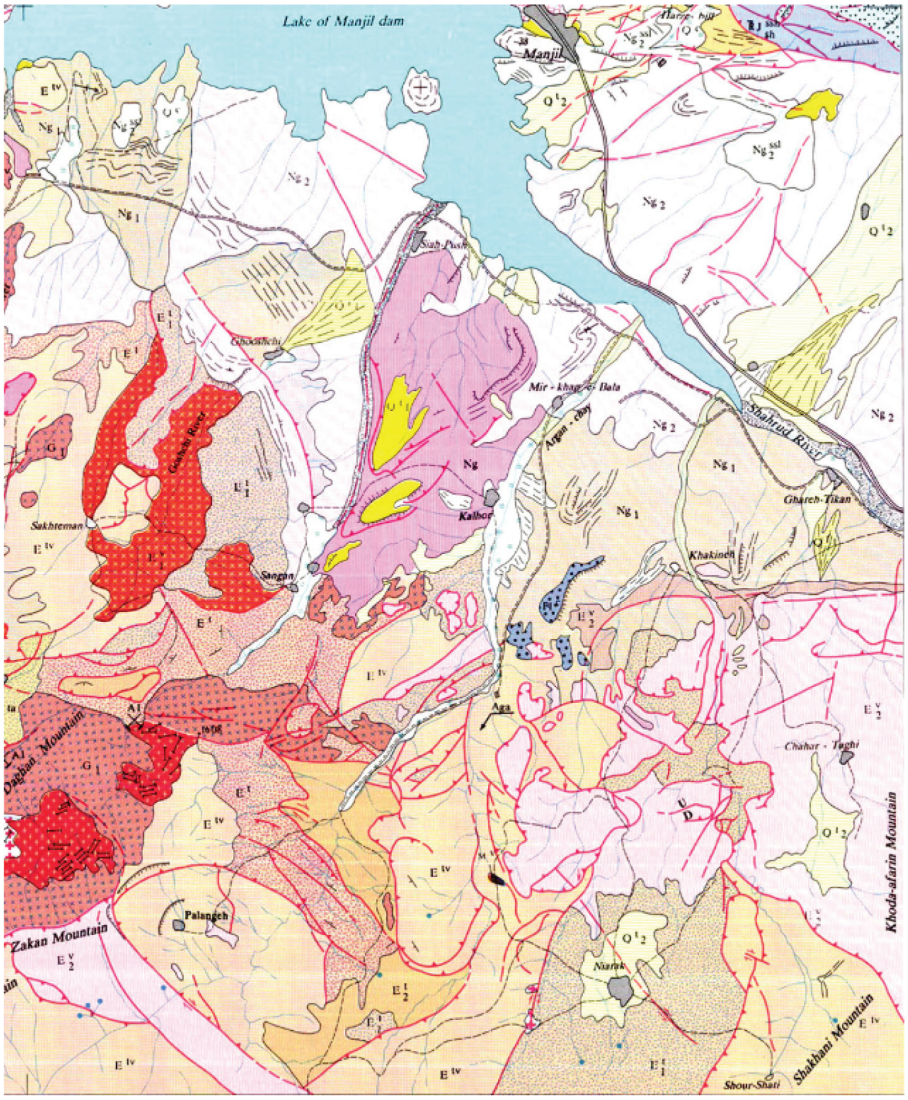

Figure 3: Geological map of the study area.

Discussion

Indirect Extraction of Lineaments

Extraction Based on the Spanning Tree Algorithm Method

In this study, method of semi-automatic extraction based on the spanning tree algorithm method has been used to determine the lineament of pixels as an array by estimating local variations of ash values in a digital image. There are some reasons behind choosing the following method:

First of all, after the extraction of lineaments of each map, they were applied to the software environment as a layer detection and repetitive lineaments were deleted. Then the azimuth values and the length of each lineament was determined. The azimuth values were plotted on the Rose diagram to analyze the orientation of the lineaments and the histogram of their length to investigate the first descriptive-statistical length of the lineaments. For investigating the lineaments of the study area (south east of Zanjan) a general perspective and a fault map (Figure 4) were used and it was determined that the highest density of faults can be found in the southwestern part of the area. In Northeastern and central parts of the study area, the abundance of faults is less frequent. According to the Rose diagram, the general trend of the study area is the faults in the northeast-southwest in which the N60E to N70E are the most frequent trend and N80E to N90E as well as the N40E to N70E are also abundant.

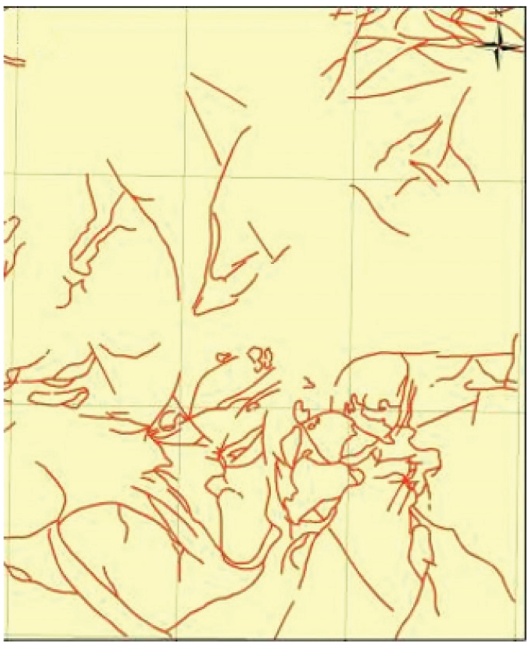

Figure 4: Faults map of study area.

Lineament Extracted from Landsat Images

After the extraction of lineaments, for Landsat7 images with a resolution of 30 m and for bands 1, 2, 3, 4, 5 and 7, six maps were obtained that were combined with the lineaments of panchromatic band or Landsat band 8 and their repetitive lineaments were removed. To determine the main orientation of the lineaments, the final map was drawn (Figure 5). Rose diagram (azimuth-lineament length) shows the maximum orientation in the S40E to S50E.

The geometric map of the region can be used to justify the lineament images obtained in Figures 3, 4 and 5.

Extracted Lineaments from Height Shadow Pattern

For the extraction of lineaments by the use of height shadow pattern, artificial light azimuths 0°, 45°, 90°, 135°, 180°, 235°, 270°, and 315° were used. First, by extracting the lineaments, eight maps were obtained in eight different azimuths. Second, the non-structural lineaments of each map were deleted and all eight maps were merged into groups of two and their repetitive lines were eliminated. Third, the final lineament map was depicted from the height shadow pattern (Figure 6). Finally, by obtaining the extracted lineament maps from the height shadow models and based on the above-mentioned maps, it can be assumed that the maximum density of the lineaments is generally located in the centre and northwest of the study area.

Figure 5: Extracted lineament map from Landsat7 satellite image.

Extraction and Analysis of the Final Lineament Map

After extracting all the lineaments from two different sources which contained some information about the complications of the earth surface and altitude, these maps were combined in the software environment and the associated lineaments were linked together and the repetitive ones were also deleted. For the local analysis of the lineaments in the study area, the density of the lineaments was determined in the final map (Figure 7).

In the final lineament map of the study area that was obtained from the integration of the final map of the Landsat images and the final map of the height shadow patterns, the dominant trend which has the most frequency among lineaments is S40E to S70E.

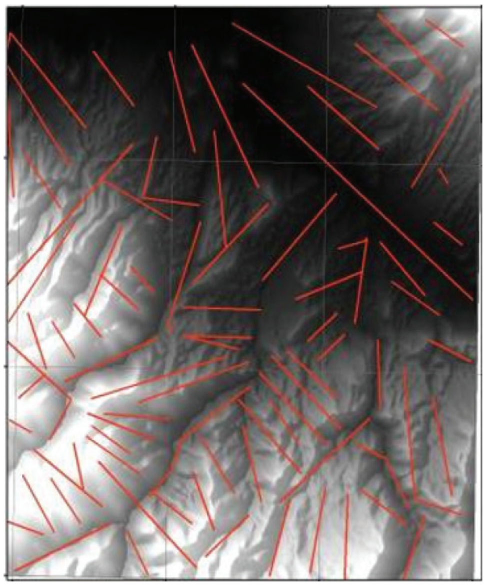

Figure 6: Extracted lineament map from height shadow patterns.

Figure 7: Final lineament map.

Folds

Folds are among the special structures that are very common in deformed rocks and plate-shaped structures that undergo a formable deformation and affect one or more layers in all studying scales. Geometry, kinematic dynamics and dynamics of folds always play an important role in understanding deformation events in orogeny belts and recognizing their space-time pattern in order to identify this part of the Earth's lithosphere. In most of these stereonets (except for a few cases where the folds are overturned and the axes of both edges are in one direction), the axes are concentrated in two distinct points that represent the angular hinges of the folds which is also a characteristic of Chevron folds. Recorded data show a wide range of geometric elements orientation, but most of the data (about 55%) are located in the area of steeply inclined-upright and sub horizontal-gently plunging folds (Figure 8), so that folds are in two categories as close (52%) and open (39%), (Figure 8). Rickard's triangular diagram (1971) may have a better application than triangular graphs. Hence, by recording the data of the slope of axial surface and the inclination of the fold hinges, it is concluded that even if they have a scattered distribution but they are classified in three groups of horizontal, upright, and curved folds (Figure 9).

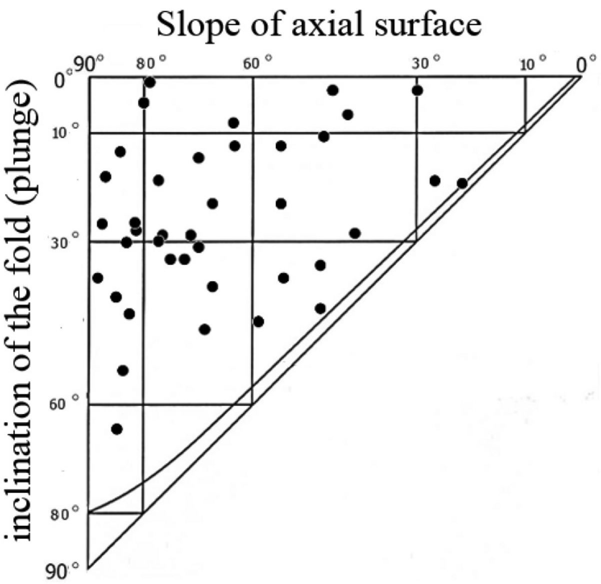

Figure 8: Mapping the slope of axial surface and the inclination angle of the fold hinge line of the study area on the graph for spatial understanding and recognizing the fold types (Rickard, 1971).

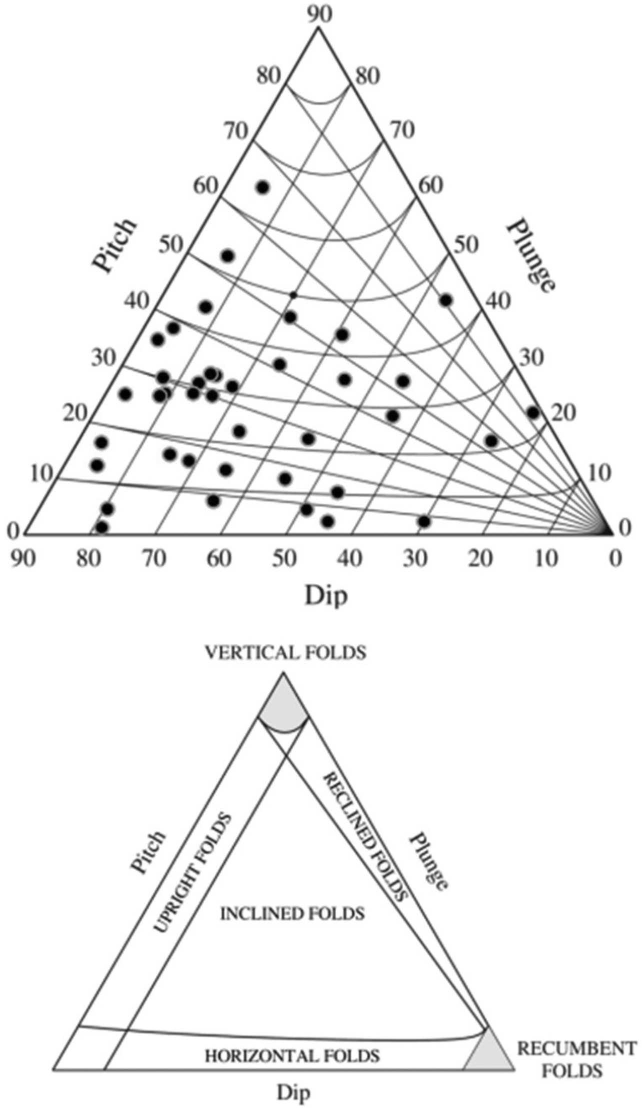

Figure 9: Corresponding diagram of the study area's folds based on Rickard's classification (1971).

The examined folds of this study were located at 39 points the results of which are shown in Table 1.

The equal area network has presented the axis of pole points for folds 1 and 2, which confirms the above-mentioned results (Figure 10). Figure 11 illustrates the rose diagram of dip and strike directions of the plates.

According to the Rose diagram, the maximum orientation and the slope of the axial surface of the folds in the study area with a mean slope of 66 degrees have been developed in the directions of 283°, 332°, 152°, and 312° which are in line with the structural pattern of structural area and tectonics of Western Alborz. The data taken from the folds of the region and the plunge of fold hinges are shown in the Rose diagram and the polar focus graph (Figure 12). Based

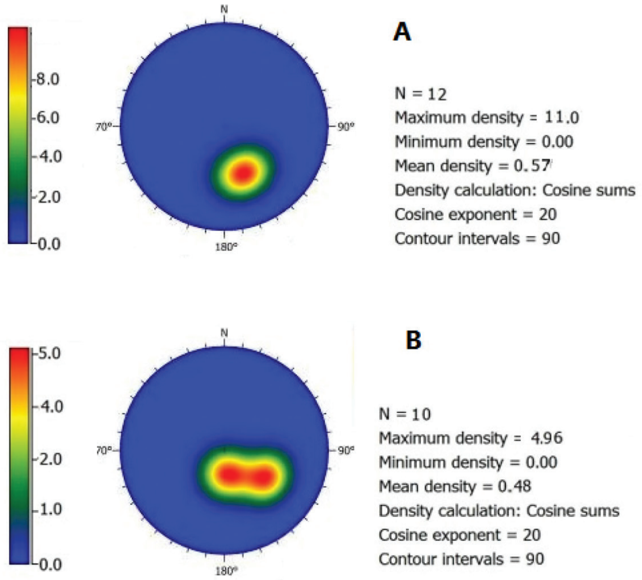

Figure 10: The equal area network, focusing on the axes of the pole points for folds 1 and 2.

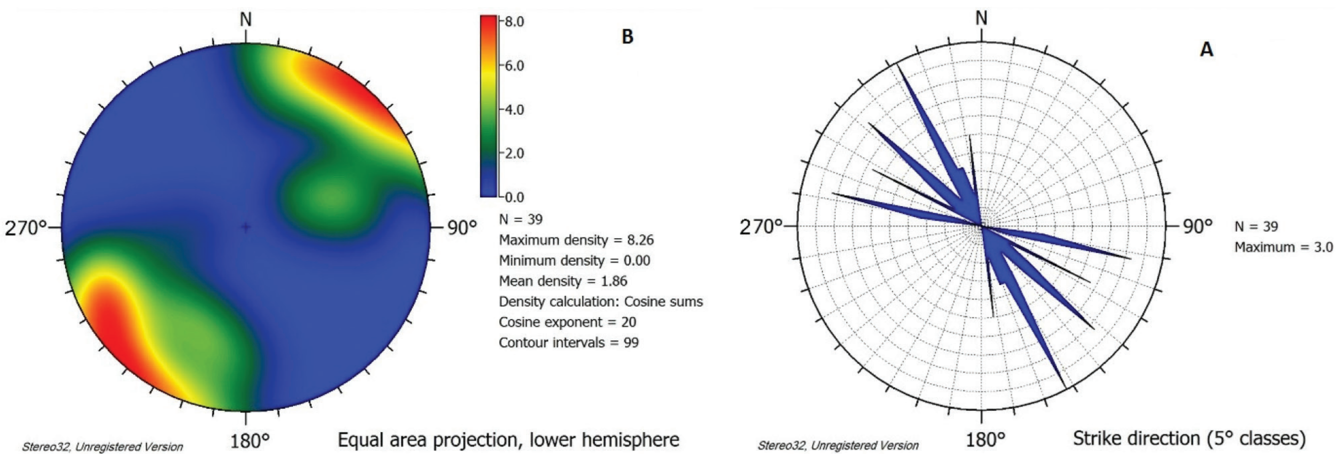

Figure 11: (A) Rose diagram and (B) polar focus of the axial levels in the study area's folds.

Table 1: Geometric characteristics of folds

Fold number	*Fold shape*	*Median angle*	*Folding angle*	*Compression*	*Axis*	*Axial level*
FO_1	Anticline	108	72	Open	14.134	161.64 NE
FO_2	Anticline	75	105	Open	31.166	154.71 NE
FO_3	Anticline	105	75	Open	22.348	104.55 SW
FO_4	Anticline	105	75	Open	14.347	170.55 SW
FO_5	Anticline	109	71	Open	36.109	115.88 SW
FO_6	Syncline	118	62	Open	16.114	120.71 NE
FO_7	Syncline	102	78	Open	65.162	149.84 NE
FO_8	Anticline	108	72	Open	47.169	150.69 NE
FO_9	Anticline	103	77	Open	22.163	174.22 NE
FO_{10}	Anticline	118	62	Close	03.153	331.30 SW
FO_{11}	Anticline	52	128	Close	44.288	298.82 NE
FO_{12}	Anticline	65	115	Close	21.318	158.27 SW
FO_{13}	Anticline	107	73	Open	03.174	171.45 NE
FO_{14}	Anticline	81	99	Open	01.161	161.79 NE
FO_{15}	Syncline	57	123	Close	08.331	278.64 NE
FO_{16}	Anticline	112	68	Open	29.157	150.77 NE
FO_{17}	Anticline	95	85	Open	16.277	280.78 NE
FO_{18}	Anticline	104	76	Open	30.326	139.78 NE
FO_{19}	Syncline	20	160	Close	11.351	166.46 SW
FO_{20}	Syncline	111	69	Open	17.283	284.87 SW
FO_{21}	Syncline	161	19	Soft	05.167	148.80 SW
FO_{22}	Anticline	142	38	Soft	39.133	137.85 SW
FO_{23}	Anticline	149	31	Soft	32.120	310.74 SW
FO_{24}	Anticline	159	21	Soft	53.163	152.83 SW
FO_{25}	Anticline	153	27	Soft	28.348	281.81 SW
FO_{26}	Syncline	107	73	Open	26.128	127.88 NE
FO_{27}	Syncline	91	89	Open	33.302	295.75 SW
FO_{28}	Syncline	95	85	Open	29.307	283.73 SW
FO_{29}	Anticline	114	66	Open	23.344	154.67 NE
FO_{30}	Anticline	151	29	Soft	29.288	159.43 SW
FO_{31}	Anticline	102	78	Open	06.283	288.49 NE
FO_{32}	Syncline	107	73	Open	13.307	308.84 SW
FO_{33}	Syncline	79	101	Open	30.335	130.82 NE
FO_{34}	Anticline	149	31	Soft	27.316	312.81 NE
FO_{35}	Anticline	162	18	Soft	44.110	279.59 NE
FO_{36}	Anticline	144	36	Soft	38.321	142.66 SW
FO_{37}	Syncline	98	86	Open	36.162	131.54 NE
FO_{38}	Anticline	92	88	Open	35.148	314.46 NE
FO_{39}	Anticline	156	24	Soft	46.292	115.46 NE

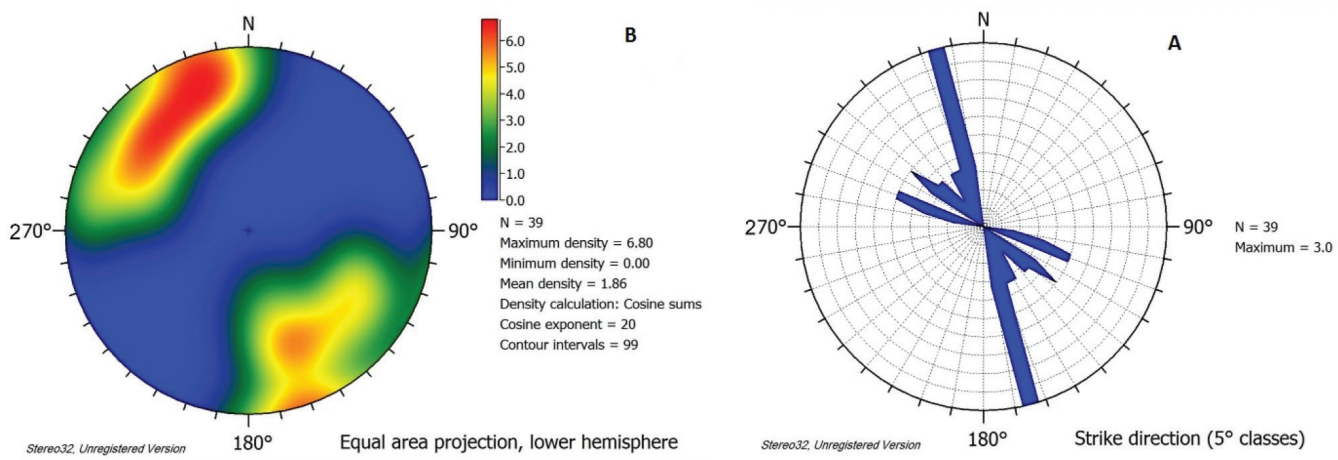

Figure 12: (A) Rose diagram and (B) Stereonet polar focusing process and the plunge of the study area's fold hinges.

on the obtained data from the graphs, most of the hinges have been developed in the direction of 455° and 165° which means the average angle of the fold hinges is 26 degrees.

Faults

The most obvious expression of fragile deformation in the earth's crust are faults. Faults are fractures that appear on all scales from microscopic to large scale which can be in the form of a plate or shear zone. The faults of this region operate with three main mechanisms at 10 to 15 kilometres of crust; the normal fault with a 90-degree angle, reverse fault with a 90-degree angle, strike-slip fault with a 0-degree angle, and oblique-slip faults with a 0 to 90-degree angle. Polar Stereonet of fault planes was plotted based on the data obtained from geometric characteristics of the fault planes and shear fractures in the study area. According to the mentioned chart, the mean angle of the slope of the fault planes is 57.7 degrees and most of the fault planes are inclined in two directions of northeast and southwest (Table 2 and Figure 13).

In the study area there are reverse and normal faults, the majority of which are reverse. In some situations, normal and reverse faults are conjugated and they can be used in estimating the stress field since the intersection of the faults is in accordance with the intermediate principal stress (2σ). In addition, the bisector of the acute angles and oblique angles of this intersection of fault (or fracture) is in accordance with the maximum principal stress (1σ) and the minimum principal stress (3σ), and the slip along with 2σ equates zero (Figure 14).

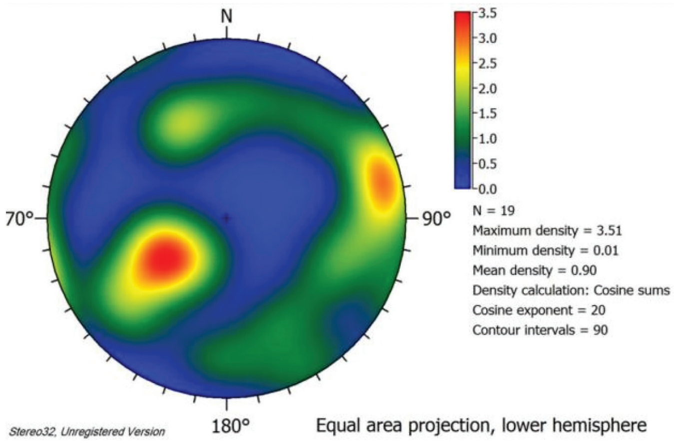

Figure 13: Polar Stereonet of fault planes in the study area.

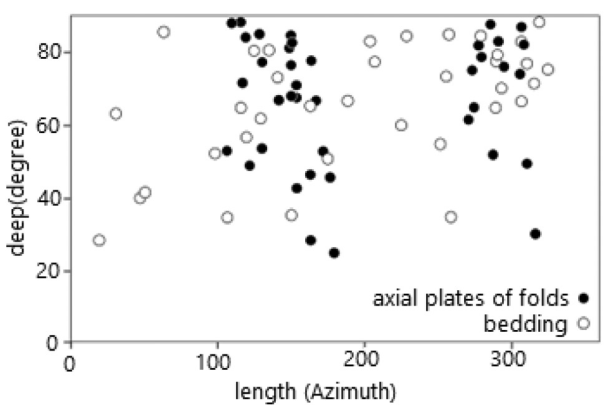

Figure 14: Testing the relationship between geometric characteristics of the axial surface of the faults and the bedding planes of the study area.

Conclusion

Investigating the study area has shown the following results. This area is located in the western part of the

Table 2: Size of the fault plates in the studied area

Orientation	*Deep (degree)*	*Length (Azimuth)*
NE	55	144
SW	55	100
NE	67	140
NE	67	092
NW	83	062
NW	53	025
NW	22	125
NW	30	155
SW	78	167
SW	82	170
SE	45	065
SW	78	160
SE	88	022
NW	55	062
SE	52	064
NW	65	009
NE	37	150
NE	35	140
SW	63	133

Chinese belt and Alborz, most of the faults are reverse and their general trend is northwest-southeast. In the study area, using the information obtained from desert harvesting related to the edges of the folds on the lower hemisphere of the equal aria network (Schmidt network) as polar concentrations and then the axis and the axial surfaces of all the folds were drawn in which the dominant trend is NW-SE and this trend complies with the structural process of the Western Alborz. During the geometric analysis of the folds, using the diagrams based on the slope of the axial surface and the plunge of the fold hinges, they are generally classified as gently to moderate plunging and steeply inclined folds. Depending on the interlimb angle and the angle of folds, most of the mentioned folds are asymmetrical and semi-circular; they are often in the category of open folds. The dispersion of data can be due to the fact that the geometry of folds has been altered due to subsequent deformation phases which both influenced the orientation of geometric elements of folds and their degree of cylindricality.

By studying Fold style elements on a folded surface (Twiss, 1988), which is the Appearance ratio (amplitude ratio/half-wavelength), the compression and rounding were obtained for some of the folds. According to the study analysis, the folds are in the category of large and semi-angled folds. Thickness data of some folded layers (vertical thickness or axial thickness) were written on Ramsay's (1967) classification diagrams which indicated that most of the folds were in category 1, especially B1 which can be indicative of the dominant buckling-flexural slip mechanism in them. Based on the evidence, the layers are not folded in the entire region and in some parts the regular layers are visible. Now, the question is whether these layers have a definite relationship with the folds and why they were not subject to folding like other units?

In order to investigate the relationship between the slope and the axial length of the region's folds and the slope and the length of the layers in the study area, the obtained information is shown in Figure 13, which shows the longitudinal axis of this chart i.e. the length of layering and axial surfaces of the folds in degrees and as an azimuth; and its transverse axis is the slope of the parameters in degrees. The data mapping of these two parameters shows a meaningful relationship. The proximity between the obtained data from the geometric characteristics of these two parameters indicates that layers that do not show any kind of folding on the scale of outcrops are also part of the whole system of folding in the study area and they can also be indicative of different degrees of folding (Ramsay and Huber, 1987; Price and Cosgrove, 1990). Faulting and erosion can also be the factors that prevent the folding of layers in some outcrops. Characteristics of plate tectonics play an important role in the expansion of magmatic activity and intrusive masses in the western Alborz which is part of Alpine orogeny and finally enters Turkey. The structural zone of the western Alborz extends along Turkey towards the Mulas Trench Caucasus Basin in the eastern part of the Molas Caucasus Basin of Turkey (Ershov et al., 2003). However, the interpretation of the tectonic transformation in the western Alborz region and the Tertiary magmatic activity of this area have been carried out in two local and regional scales (Lescuyer and Riou, 1976; Berberian, 1981; Allen et al., 2003).

According to the previous studies, three important models have been presented to introduce the tectonic and magmatic Tertiary developments in Western Alborz (Berberian, 1981; Allen et al., 2003). The second model refers to the existence of thermal domes under the Iranian block in western Alborz and in Tertiary era (Lescuyer and Riou, 1976). The third model is in contrast with the first model that considers magmatic-tectonic activity as a result of a collision, but the followers of this model have not provided strong evidence so far. In the study area, most of the previous studies were randomly taken from different stratigraphy layers based on geochemical or estimated analyses on the collected samples and unfortunately, local and global tectonic interpretations with respect to desert and geochemical data are not clear and accurate. Although, in the Tarom area of the western Alborz zone, the sequence of Lava deposits and Eocene pyroclastics with the name of Karaj Formation with a depth of more than 3,800 metres has sub-alkaline outcrop properties, but it is discontinued by intrusive lower Oligocene magmatic activities. This mentioned tectonic and lithology sequence has an astonishing resemblance to some parts of Turkey such as Aliağa-Foça in the western part of Anatolia, Turkey and Yozgat, Sulakyuat, Bayindir-Hamit and Kesikköprü in Central Anatolia (Boztuğ, 1998). The sedimentary-Eocene sequence in the study area includes andesite, trachy andesite, dacite, rhyolite, welded tuff, shear tuff, lichen tuff, ignimbrite, and acidic tuff.The activity of Eocene lava in the study area has been controlled by weak areas with a similar northwest-southeast trend. In fact, these weak areas are shear zones that are formed perpendicular to the compression zones with a northeast-southwest trend which are formed by the collision of Iranian-Arabian blocks.

References

Adib, A., MirzaeiIlani, S., Shoaei, G. and P. Afzal (2017). Determination of a Conceptual Model for the Structural Features and Pb–Zn Mineralization in the North of Behabad Fault Zone, Central Iran. *Iranian Journal of Earth Sciences*, **9(2):** 0-0.

Alavi, M. (1991). Sedimentary and structural characteristics of the Paleo-tethys remnants in northeastern Iran, *Geological Society of America Bulletin* 103: 983-992.

Alavi M (1996) Tectonostratigraphic synthesis and structural style of the Alborz Mountain system in northern Iran. *Journal of Geodynamics*, **21:** 1-33.

Alavi, M., Eftekhar-Nezhad, J., Haghipour, A., Hajian, J., Hirayama, K., Hushmand-Zadeh, A., Nabavi, M.H., Samimi, M., Stöcklin, J., Valeh, N. and M. Zahedi (1969). Explanatory text of the Zanjan Quadrangle Map, 1:250000. Geological Survey of Iran, Geological Quadrangle D4: 1-61.

Alavi, M., Vaziri, H., SeyedEmami, K. and Y. Lasemi (1997). The Triassic and associated rocks of the Nakhlak and Aghdarband area in central and northeastern Iran as remnent of the southern turanian active continental margin. *Geological Society of America Bulletin*, **109:** 1563-1575.

Allen, M.B., Ghassemi, M.R., Shahrabi, M. and M. Qorashi (2003). Accommodation of late Cenozoic oblique shortening in the Alborz range, northern Iran. *Journal of Structural Geology*, **25(5):** 659-672.

Axen, G.J., Lam, P.S., Grove, M., Stockli, D.F. and J. Hasssanzadeh (2001). Exhumation of the west-central Alborz Mountain, Iran, Caspian subsidence, and collision-related tectonics. *Geological Society of America*, **29:** 559-562.

Bayet-Goll, A., Moussavi-Harami, R. and A. Mahboubi, A. (2016). Ichnotaxonomic analysis and depositional controls on the carbonate ramp ichnological characteristics of the Deh-Sufiyan Formation (Middle Cambrian), Central Alborz, Iran. *Iranian Journal of Earth Sciences*, **8(2):** 102-124.

Bazargani-Guilani, K., Parchekani, M. and M.A. NekouvaghtTak (2008). Mineralization in the Taroum mountains, View to Barik-Ab Pb-Zn (Cu) deposit, Western Central Alborz, Iran. WSEAS Conferences in Cambridge, **1:** 55-63.

Berberian, M. and G.C. King (1981). Towards a palaeogeography and tectonics evolution of Iran. *Canadian Journal of Earth Sciences*, **18:** 210-265.

Boztuğ, D. (1998). Post-collisional Anatolian plutonism, Turkey. *Turkish Journal of Earth Sciences*, **7:** 145-165.

Donath, F.A. and R.B. Purker (1964). Folds and Folding. *Geological Society of America Bulletin*, **75:** 45-62.

Ershov, A.V., Brunet, M.F., Nikishin, A.M., Bolotov, A.N., Nazarevich, B.P. and M.V. Korotaev (2003). Northern Caucasus basin: Thermal history and synthesis of subsidence models. *Journal of Sedimentary Geology*, **156:** 95-118.

Ehteshami-Moinabadi, M. (2016). Possible Basement Transverse Faults in the Western Alborz, Northern Iran. *Journal of Sciences, Islamic Republic of Iran*, **27(4):** 329-342.

Guest, B., Axen, G., Lam, P.S. and J. Hassanzadeh (2006). Late Cenozoic shortening in the west-central Alborz Mountains, northen Iran, by combined conjugate strike-slip and thin-skinned deformation. *Geological Society of America*, **2:** 35-52.

Guest, B., Guest, A. and G. Axen (2007). Late Tertiary tectonic evolution of northern Iran: A case for simple crustal folding. *Journal of Global and Planatary Change*, **58:** 435-453.

Lescuyer, J.L. and R. Riou (1976). Geologiede la re'gion de Mianeh (Azarbaijan), contribution al'etude du volcanisme tertiaire de l'Iran. N.I.O.C. (National Iranian Oil Company), 1977. Geological map of Iran, 1:1000000.

Mattei, M., Cifelli, F., Alimohammadian, H., Rashid, H., Winkler, A. and L. Sagnotti (2017). Oroclinal bending in the Alborz Mountains (Northern Iran): New constraints on the age of South Caspian subduction and extrusion tectonics. *Gondwana Research*, **42:** 13-28.

Price, N.J. and J.W. Cosgrove (1990). Analysis of Geological Structures. Cambridge University Press, Great Britain.

Ramsay, J.G. (1967). Folding & fracturing of rocks. McGraw-Hill, New York.

Ramsay, J.G. (1974). Development of chevron folds. *Geological Society of America Bulletin*, **85:** 1741-1754.

Ramsay, J.G. and M. Huber (1987). The Techniques of Modern Structural Geology. Academic Press, **2:** 309-700.

Rickard, M.J. (1971). A classification diagram for fold orientation. *Geological Magazine*, **108:** 23-26.

Şengör, A.M.C. (1990). A new model for the late Paleozoic–Mesozoic tectonic evolution of Iran and implications for Oman. *In:* The Geology and tectonics of the Oman region. *Special Publication of Geological Society of London*, **49:** 797-831.

Stocklin, J. (1974). Northern Iran; Albrouse Mountains. *In:* Mesozoic-Cenozoic Orogenic Belt. *Special Publication of Geological Society of London*, **4:** 213-234.

Stoklin, J. (1968). Structural history and tectonics of Iran: A review. *American Association of Petroleum Geologists Bulletin*, **52(7):** 1229-1258.

Twiss, R.J. (1988). Description and classification of folds in single surfaces. *Journal of Structural Geology*, **10:** 607-623.

Zanchi, A., Berra, F., Mattei, M., Ghassemi, M.R. and J. Sabouri (2006). Inversion tectonics in central Alborz, Iran. *Journal of Structural Geology*, 1-15.